

# Dicke superradiance in ordered lattices: role of geometry and dimensionality

Eric Sierra, Stuart J. Masson, and Ana Asenjo-Garcia\*

*Department of Physics, Columbia University, New York, NY 10027, USA*

(Dated: May 3, 2022)

Many-body superradiance in ordered atomic arrays is a phenomenon where atomic synchronization gives rise to a burst in photon emission. This superradiant burst only occurs if there is one – or just a few – dominant decay channels. By mapping the question of whether many-body superradiance occurs into a simple algebraic equation, we demonstrate that it exists in arrays of any dimensionality, as interference in photon emission leads to the preeminence of certain channels over others. In atomic chains superradiance occurs only below a critical interatomic distance, which we derive analytically. Increasing the array dimensionality leads to a critical distance that scales with system size: sub-logarithmically for 2D, and seemingly faster than that for 3D lattices. We perform calculations for both infinite and finite systems, the latter by employing a highly-efficient algorithm with a computational complexity that scales only linearly with system size, which enables us to study very large arrays. Our results provide a guide to explore this many-body phenomenon in state-of-the-art experimental setups.

Collective emission has been a fundamental problem in quantum optics since the notion was introduced by Dicke in 1954 [1]. Dicke realized that proximate atoms must interact via shared electromagnetic field modes, fundamentally altering their optical properties. He considered the case of a fully excited ensemble of emitters located at a single point. In stark contrast to the exponentially-decaying pulse emitted by independent (i.e., far-separated) particles, emitters at a point synchronize, locking in phase as they decay, and emitting a short burst of light that initially rises in intensity [1–4] [see Fig. 1(a)]. This “superradiant burst” has become a hallmark of collective phenomena in quantum optics and has been observed in a variety of physical systems [5–11]. Generally, experiments are performed in dense disordered systems, where interparticle separations can be very small, or in a cavity, where the restriction of the field to a single confined mode emulates the condition of atoms at a point.

In extended and ordered arrays in free space, the geometry and dimensionality of the lattice define the atomic decay properties due to position-dependent dipole-dipole interactions. For example, in ordered arrays with sub-wavelength interatomic separation, subradiant states with an extremely enhanced lifetime emerge [12–14]. These can be used to guide light as “atomic waveguides” [15–17] or “atomic dielectrics” [18–21], and to improve the fidelity of protocols for quantum information storage [16, 22, 23] and metrology [24, 25], among other applications. Arranging single atoms in ordered patterns has become an experimental reality [26–34]. Interatomic separations in these platforms can be small enough that the optical response is strongly modified by photon interference effects. Predictions that a two-dimensional array acts as an atomically-thin mirror have been demonstrated [35–37], and site-dependent frequency shifts due to dipole-dipole interactions have been measured [38].

The role of geometry in many-body (i.e., many-photon,

or “Dicke”) superradiance has not yet been completely elucidated. The introduction of spatially-varying dipole-dipole interactions to Dicke’s original model causes position-dependent frequency shifts that lead to dephasing, damping superradiance [39, 40]. This is significant in disordered systems, and points to the key role of geometry, as it determines the spatial pattern of these frequency shifts [41–43]. However, dephasing is reduced in large ordered arrays, as the frequency shifts are predominantly homogeneous [3, 4, 40]. In such systems, the primary source of dephasing is competition between multiple decay channels [44, 45].

Here, we study the onset of superradiance in multiple lattices of different dimensionalities. To do so, we harness a technique derived in our previous work [45]. It enables us to deduce the minimal conditions for Dicke superradiance without calculating the full dynamical evolution of the system, simply by analyzing the statistics of the first two emitted photons [45]. We show that the critical distance beyond which Dicke superradiance disappears increases with array dimensionality. It saturates to a certain bound in one-dimensional (1D) arrays, which we obtain analytically for infinite chains. It increases sub-logarithmically with atom number in two-dimensional (2D) lattices, and more rapidly in three-dimensional (3D) ensembles. We also analyze the role of lattice geometry and polarization of the atomic transition. In contrast to Dicke’s original work, which assumes that all atoms are confined to a volume of dimensions much smaller than the transition wavelength, we show that superradiance survives in arrays where the *smallest* interparticle distance is larger than a wavelength.

We consider ordered arrays of  $N$  two-level atoms of resonance frequency  $\omega_0$ , resonance wavelength  $\lambda_0 = \omega_0/c$ , and spontaneous emission rate  $\Gamma_0$  arranged at positions  $\{\mathbf{r}_i\}$ . We define  $d$  as the smallest interatomic distance in the set  $\{|\mathbf{r}_i - \mathbf{r}_j|\}$  (see Fig. 1)). The atoms interact via the electromagnetic field, which is traced out using

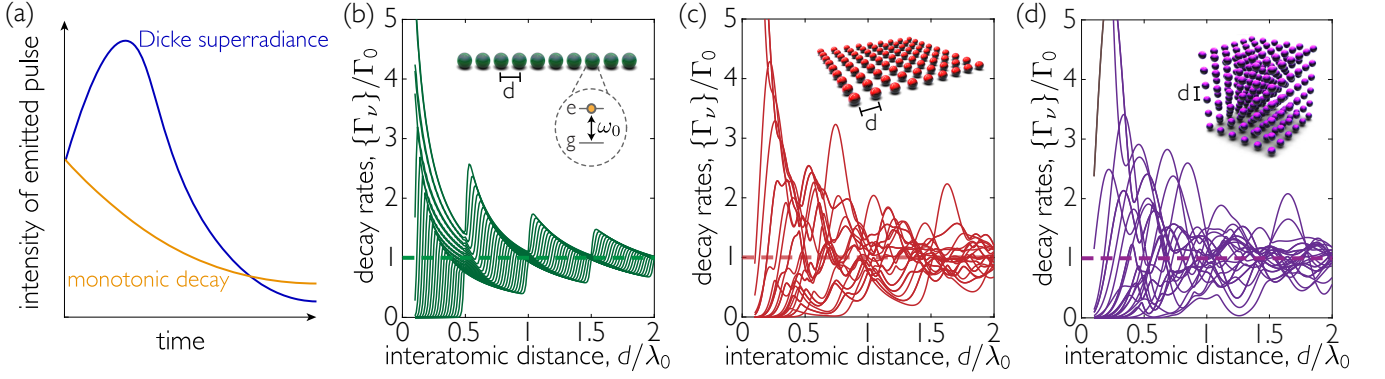


FIG. 1. (a) Schematic of Dicke superradiance, which results from atomic correlations and leads to a burst in the emitted intensity, in contrast to the monotonic decay from uncorrelated atoms. In ordered arrays, the interatomic distance controls the crossover between the two regimes. (b-d) Collective decay rates as a function of interatomic distance  $d$  for atomic arrays of different dimensions. (b)  $N = 25$  atoms form a 1D array, and the transition polarization is perpendicular to the chain. (c)  $N = 5^2 = 25$  atoms form a 2D lattice with polarization axis out-of-plane. (d)  $N = 3^3 = 27$  atoms are arranged in a 3D lattice, with polarization axis aligned with one of the main axes of the array.

a Born-Markov approximation [46, 47]. The atomic density matrix,  $\rho = |\psi\rangle\langle\psi|$ , evolves according to the master equation

$$\dot{\rho} = -\frac{i}{\hbar} [\mathcal{H}, \rho] + \sum_{\nu=1}^N \frac{\Gamma_\nu}{2} \left( 2\hat{O}_\nu \rho \hat{O}_\nu^\dagger - \rho \hat{O}_\nu^\dagger \hat{O}_\nu - \hat{O}_\nu^\dagger \hat{O}_\nu \rho \right). \quad (1)$$

In the above expression, the Hamiltonian is given by

$$\mathcal{H} = \hbar \sum_{i=1}^N \omega_0 \hat{\sigma}_{ee}^i + \hbar \sum_{i,j=1}^N J^{ij} \hat{\sigma}_{eg}^i \hat{\sigma}_{ge}^j, \quad (2)$$

where  $\hat{\sigma}_{ge}^i = |g_i\rangle\langle e_i|$  is the atomic lowering operator for atom  $i$ , with  $|g_i\rangle$  and  $|e_i\rangle$  the atomic ground and excited state respectively. The Lindblad operator has been diagonalized into the action of  $N$  collective jump operators,  $\{\hat{O}_\nu\}$  with decay rates  $\{\Gamma_\nu\}$  [48, 49]. These are found as the eigenstates and eigenvalues of the dissipative interaction matrix  $\mathbf{\Gamma}$  with elements  $\Gamma^{ij}$ . The coherent and dissipative interaction rates read

$$J^{ij} - i \frac{\Gamma^{ij}}{2} = -\frac{\mu_0 \omega_0^2}{\hbar} \boldsymbol{\varphi}^* \cdot \mathbf{G}_0(\mathbf{r}_i, \mathbf{r}_j, \omega_0) \cdot \boldsymbol{\varphi}, \quad (3)$$

where  $\boldsymbol{\varphi}$  is the dipole matrix element of the atomic transition and  $\mathbf{G}_0(\mathbf{r}_i, \mathbf{r}_j, \omega_0)$  is the propagator of the electromagnetic field between points  $\mathbf{r}_i$  and  $\mathbf{r}_j$ . Each jump operator represents the emission of a photon into a particular decay channel (with some specific far-field profile). Jump operators act on all atoms, and can be expressed as superpositions of atomic lowering operators,  $\hat{O}_\nu = \sum_{i=1}^N \alpha_{\nu,i} \hat{\sigma}_{ge}^i$ , where  $\alpha_{\nu,i}$  represents some spatial profile over the ensemble.

Following our previous work [45], we define the minimal condition for Dicke superradiance to have the first

photon enhance the subsequent one or, equivalently, to have a greater than unity second-order correlation function at  $t = 0$ . The correlation function  $g^{(2)}(0)$  can be calculated exactly for an initially fully-inverted state and yields [45]

$$g^{(2)}(0) = \frac{\sum_{\nu,\mu=1}^N \Gamma_\nu \Gamma_\mu \langle \hat{O}_\nu^\dagger \hat{O}_\mu^\dagger \hat{O}_\mu \hat{O}_\nu \rangle}{\left( \sum_{\nu=1}^N \Gamma_\nu \langle \hat{O}_\nu^\dagger \hat{O}_\nu \rangle \right)^2} = 1 + \frac{1}{N} \left( \text{Var} \left[ \frac{\{\Gamma_\nu\}}{\Gamma_0} \right] - 1 \right), \quad (4)$$

where  $\text{Var}\{\{\Gamma_\nu\}/\Gamma_0\} = (1/N) \sum_{\nu=1}^N (\Gamma_\nu^2 - \Gamma_0^2)/\Gamma_0^2$  denotes the variance of the decay rates.

The problem of identifying the minimal conditions for a superradiant burst is thus reduced to finding the eigenvalues of the dissipative interaction matrix, an operation that scales polynomially with atom number. Taking advantage of the symmetries of the problem, we calculate  $g^{(2)}(0)$  without diagonalizing the matrix, requiring only  $O(N)$  steps (see Supplemental Material for full details [50]). This allows us to study arrays of  $N \simeq 10^7$  atoms.

Figure 1(b-d) shows the decay rates as a function of interatomic distance  $d$ , for all array dimensionalities. As  $d$  increases, the decay rates cluster around the single-atom decay rate  $\Gamma_0$ , decreasing the variance. However, there are ‘‘revivals’’ or ‘‘geometric resonances’’ at particular distances due to long-range interactions arising from  $1/r$  terms in the Green’s tensor [51, 52], which prevent the second-order correlation function from decreasing monotonically with  $d$  [50]. This means that establishing regions of superradiance is non-trivial. As  $d$  is increased, superradiance can be lost, but then re-established by a geometric resonance [45]. Here, we define  $d_{\text{critical}}$  as the

largest interatomic distance at which the array can produce a superradiant burst (there can thus be distances  $d < d_{\text{critical}}$  where a superradiant burst is not produced).

As we demonstrate below, the critical distance in large 1D arrays saturates to  $d_{\text{critical}}^{\text{1D}} = 0.3\lambda_0$ . Jump operators in infinite 1D arrays can be written as spin waves  $\hat{O}_{k_z} = (1/\sqrt{N}) \sum_{i=1}^N e^{ik_z z_i} \hat{\sigma}_{g_e}^i$ , where we assume the array to lie along the  $z$ -axis. In the above expression,  $k_z$  is the wavevector and  $z_i$  are the atomic positions. As  $N \rightarrow \infty$ , the finite set  $\{k_z\}$  becomes a continuum. The decay rates can be calculated analytically for a perfect array by taking the Fourier transform of the imaginary part of the Green's function [16].

$$\frac{\Gamma_{\text{1D},\parallel}(k_z)}{\Gamma_0} = \frac{3\pi}{2k_0 d} \sum_{g_z} \left( 1 - \frac{(k_z + g_z)^2}{k_0^2} \right), \quad (5a)$$

$$\frac{\Gamma_{\text{1D},\perp}(k_z)}{\Gamma_0} = \frac{3\pi}{4k_0 d} \sum_{g_z} \left( 1 + \frac{(k_z + g_z)^2}{k_0^2} \right). \quad (5b)$$

The summations run over reciprocal lattice vectors  $g_z = n2\pi/d \forall n \in \mathbb{Z}$  that satisfy the condition  $|g_z + k_z| \leq k_0$ . The sum is thus restricted to modes that lie inside the light cone. As shown in Fig. 2(a), for  $|k_z| > k_0$ , no value of  $g_z$  satisfies the above condition, and modes are completely dark.

In the  $N \rightarrow \infty$  limit, the condition for superradiance in 1D is recast as (see Supplemental Material [50])

$$\int dk_z \frac{\Gamma_{\text{1D}}^2(k_z)}{\Gamma_0^2} > \frac{4\pi}{d}. \quad (6)$$

Integrating over the first Brillouin zone, the critical distances for both polarizations are found to be

$$d_{\text{critical}}^{\text{1D},\parallel} = 0.3\lambda_0, \quad (7a)$$

$$d_{\text{critical}}^{\text{1D},\perp} = 0.2625\lambda_0. \quad (7b)$$

We demonstrate in the Supplemental Material that the condition for superradiance is only met within the first Brillouin zone [50]. These are therefore hard bounds on superradiance for 1D arrays.

The values of  $d_{\text{critical}}$  derived in the infinite limit are corroborated by numerical calculations in finite arrays, as shown in Fig. 2(b). The critical distance saturates to the analytical solution even for modest atom numbers, and it grows smoothly with  $N$ . This occurs because the geometric resonances that suddenly modify the distribution of decay rates appear at larger interatomic distances [see Fig. 1(b)]. Parallel polarization produces higher values of  $d_{\text{critical}}$  because some operators within the light cone are subradiant, which, due to the fixed trace of  $\mathbf{\Gamma}$ , produces more superradiant operators and increases the variance [see Fig. 2(a)].

One-dimensional arrays are unique, as superradiance for two dimensions and above occurs for any distance in

the thermodynamic limit. For 2D arrays as  $N \rightarrow \infty$ , the spatial profiles of the jump operators admit a description in terms of plane waves, i.e.,  $\hat{O}_{\mathbf{k}} = (1/\sqrt{N}) \sum_{i=1}^N e^{i\mathbf{k}\cdot\mathbf{r}_i} \hat{\sigma}_{g_e}^i$ , where  $\mathbf{k}$  is a two-component wavevector that lives in the plane of the array. As in 1D, decay rates can be found analytically (see Supplemental Material [50] and Ref. [16]). The condition for a superradiant burst in 2D is [50]

$$\int d\mathbf{k} \frac{\Gamma_{\text{2D}}^2(\mathbf{k})}{\Gamma_0^2} > \frac{8\pi^2}{d^2}. \quad (8)$$

In the first Brillouin zone, the integral of the square of the decay rates for out-of-plane polarization is

$$\int \left( \frac{\Gamma_{\text{2D},\perp}(\mathbf{k})}{\Gamma_0} \right)^2 d\mathbf{k} = \frac{9\pi^2}{k_0^6 d^4} \int_0^{2\pi} d\theta \int_0^{k_0} \frac{k^5}{k_0^2 - k^2} dk, \quad (9)$$

which diverges as  $k \rightarrow k_0$ . The same is true for the integral for in-plane polarization. While we only perform the integral in the first Brillouin zone here, an identical divergence occurs for  $|\mathbf{k}+\mathbf{g}| \rightarrow k_0$  in whichever Brillouin zones

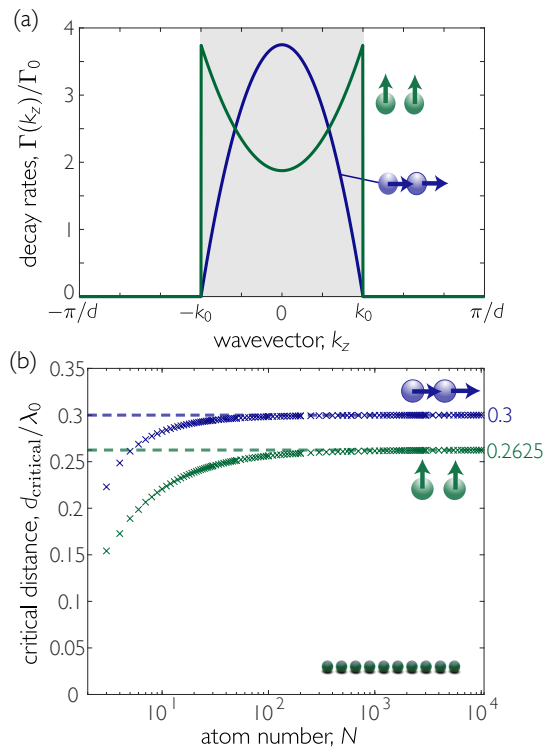


FIG. 2. The critical distance (beyond which there is no Dicke superradiance) saturates with atom number in 1D. (a) Decay rates in the first Brillouin zone, for both polarizations (parallel, in blue; and perpendicular, in green) for an infinite 1D array of  $d = 0.2\lambda_0$ . The shaded region represents the light cone, where modes are radiative. (b) Scaling of the critical distance with atom number. Dashed lines show the analytical result for  $d_{\text{critical}}$  obtained for infinite arrays [see Eq. (7)].

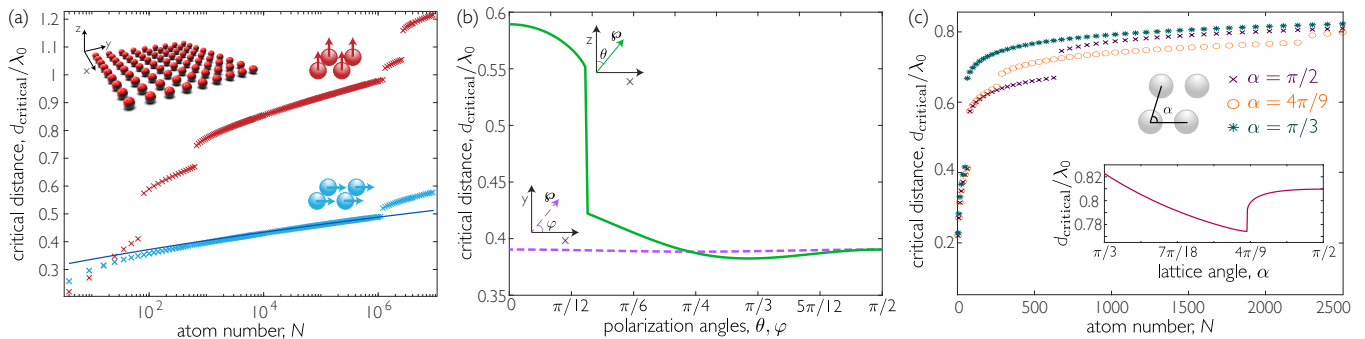


FIG. 3. The critical distance increases sub-logarithmically with atom number in 2D arrays, here shown for square 2D arrays. (a) Scaling of the critical distance with atom number for two polarizations (in the plane of the array, in blue; and out-of-plane, in red). The solid line shows a fit to the function for an infinite array, i.e., Eq. (10), for in-plane polarization with  $\alpha = 0.3247$ . (b) Critical distance as a function of polarization angle, for in-plane (purple) and out-of-plane (green) polarization, for  $N = 10^2 = 100$  atoms. (c) Scaling of the critical distance with  $N$  for square (purple crosses), rhombic (orange circles) and triangular (teal stars) lattices. (inset) Critical distance for  $N = 50^2 = 2500$  atoms in a 2D lattice as a function of lattice angle. In both plots, atoms are polarized out-of-plane.

that condition is met. We isolate the divergence by noting that, numerically, the integral scales as  $\alpha k_0^4 \ln(1/\varepsilon)$ , where  $\varepsilon \rightarrow 0$  is a small deviation from  $k = k_0$ . A large finite array of atom number  $N$  samples each dimension of the first Brillouin zone with frequency  $1/\sqrt{N}$  so, by approximating  $\varepsilon \sim 1/\sqrt{N}$ , we find the critical distances for  $d < 0.5\lambda_0$  to be [50]

$$d_{\text{critical}}^{2\text{D},\parallel} \simeq \frac{3\lambda_0}{4} \sqrt{\frac{1}{2\pi} + \frac{3\alpha}{8\pi} \ln\sqrt{N}}, \quad (10a)$$

$$d_{\text{critical}}^{2\text{D},\perp} \simeq \frac{3\lambda_0}{4} \sqrt{\frac{\alpha}{\pi} \ln\sqrt{N}}. \quad (10b)$$

The result for parallel polarization agrees with our numerical findings, as shown in Fig. 3(a). The coefficient  $\alpha = 0.3247$  is obtained by fitting up to  $N = 1000^2 = 10^6$ . Beyond that size, the critical distance lies beyond the first Brillouin zone. Fits for the perpendicular polarization disagree with numerics, for two main reasons. First, for small atom numbers (when the critical distance lies in the first Brillouin zone) the sampling error is too large. Second, for large atom numbers the critical distance lies beyond the first Brillouin zone and we should account for more terms in the sum over reciprocal lattice vectors. Nevertheless, we expect the critical distance to scale sub-logarithmically with atom number even for large interatomic distances.

We have demonstrated that in 2D the critical distance scales with system size, albeit very slowly. This, however, should not be understood as having superradiance for any distance for infinite arrays, as multiple approximations our model relies on break down in this limit. For instance, the derivation of the master equation [Eq. (1)] is done under the Born-Markov approximation, which assumes that the maximum interatomic distance is small enough that one can ignore the propagation time of photons between atoms. As  $N, d \rightarrow \infty$ , this assumption is

broken. Nevertheless, the critical distance for any large number of atoms will be significantly higher than in 1D.

While numerical calculations confirm the sub-logarithmic scaling of  $d_{\text{critical}}$ , Fig. 3(a) shows that the critical distance does not increase smoothly. This is due to the geometric resonances discussed above, which produce revivals in  $g^{(2)}(0)$  and disconnected regions of superradiance [45]. Atoms with in-plane polarization produce smaller values of  $d_{\text{critical}}$  because far-field emission is forbidden in one direction in the plane. This means that the  $1/r$  terms are only significant in one direction, diminishing revivals in  $g^{(2)}(0)$  and slowing the growth of  $d_{\text{critical}}$  with  $N$ . This is evident in Fig. 3(a), where the discontinuity for the in-plane polarized case is much smaller in size and occurs at much higher  $N$  than for the out-of-plane polarized case. As the polarization vector is rotated towards the plane, the revivals in  $g^{(2)}(0)$  diminish, until at some point they are not strong enough to produce a superradiant burst, as shown in Fig. 3(b). For small  $N$ , where the revivals are not relevant in defining  $d_{\text{critical}}$ ,  $d_{\text{critical}}$  grows faster with  $N$  for out-of-plane polarization because large numbers of subradiant operators persist to large distances in such arrays [16, 45].

As shown in Fig. 3(c), the geometry of the lattice has a minor impact on the critical distance. For large  $N$ , a triangular lattice maximizes  $d_{\text{critical}}$ , as this geometry minimizes all periodic distances between neighboring atoms. The number of discontinuities in  $d_{\text{critical}}$  changes with geometry, as seen in Fig. 3(c). For a square lattice, there are two discontinuities in the region  $d \in [0.5\lambda_0, \lambda_0]$ , one associated to the nearest neighbor distance, and one for the diagonal displacement across the unit cell. For a rhombic lattice, there are three discontinuities, as the diagonal displacements are different. For a triangular lattice, there is only one, as all distances of the unit cell are the same.

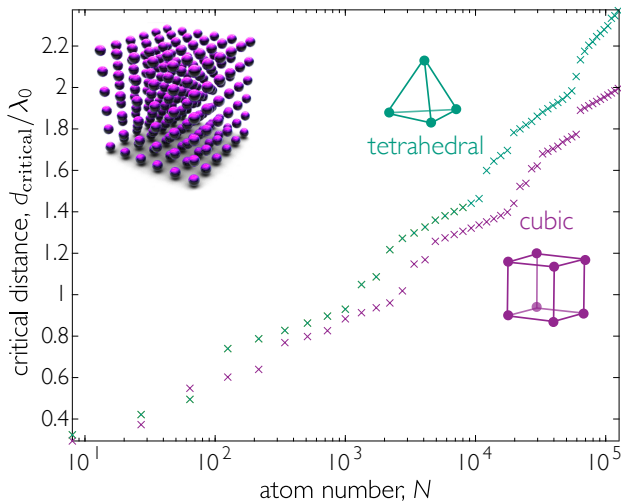


FIG. 4. The critical distance grows with atom number in 3D arrays, as shown for atoms arranged in cubic (purple) and tetrahedral (turquoise) lattices. In both cases, the transition polarization is parallel to one of the main axes of the arrays.

Three-dimensional arrays are intrinsically different from 1D and 2D: one cannot consider the infinite limit as emission into the far-field cannot happen from an infinite 3D system. Therefore, we only study finite 3D arrays in this section. Figure 4 shows that superradiance persists to much larger distances for 3D arrays than 2D arrays. Increasing dimensionality again greatly increases  $d_{\text{critical}}$ . As in 2D, the optimal geometry appears to be the one that optimizes packing efficiency and thus minimizes all displacement vectors. Here, this is the tetrahedral lattice, for which  $d_{\text{critical}} \approx 2.3\lambda_0$  for a  $N = 50^3$  array. As in 2D, there does not seem to be any saturation of  $d_{\text{critical}}$  as  $N \rightarrow \infty$ , indicating a divergent critical distance in 3D.

Finally, we note that our method is limited to identifying the minimal conditions for the presence of a burst, but not the properties of the burst. Information about, for example, the scaling of the peak emission requires a different approach [53, 54]. We also consider only the total photon emission (i.e., integrating the radiation over all directions). As we discuss in Ref. [45], a superradiant burst can be observed at distances greater than  $d_{\text{critical}}$  if emitted light is measured only in particular directions. Our algebraic technique has been recently adapted for that purpose [55].

In conclusion, we have shown that superradiant bursts can exist well beyond the regime first considered by Dicke. By calculating the maximum interatomic distance at which a superradiant burst occurs, we find that superradiance persists to much larger distances in higher-dimensional arrays, as they have a larger density of dark channels than their low-dimensional counterparts. Current state-of-the-art optical tweezer array and optical lattice experiments already operate well below these

bounds [37, 38], and superradiance could thus be observed in such systems. Arrays of solid-state emitters hosted in 2D materials [56–58] or in bulk crystals [59, 60] can also be employed to explore this physics. Our theoretical methods can be applied to studies of collective emission with atoms with more complex level structure [61–63], and atoms coupled to other reservoirs, such as nanophotonic structures [64, 65].

**Acknowledgments** – We are thankful for insightful discussions with S. Yelin and O. Rubies Bigorda. S.J.M is supported by Programmable Quantum Materials, an Energy Frontier Research Center funded by the U.S. Department of Energy (DOE), Office of Science, Basic Energy Sciences (BES), under award DE-SC0019443. E. Sierra and A.A.G acknowledge support from the A. P. Sloan Foundation, and the National Science Foundation CAREER Award (No. 2047380), respectively.

*Note added* – During the writing phase of this manuscript, we became aware of related work by F. Robicheaux [55].

\* ana.asenjo@columbia.edu

- [1] R. H. Dicke, Coherence in spontaneous radiation processes, *Phys. Rev.* **93**, 99 (1954).
- [2] N. E. Rehler and J. H. Eberly, Superradiance, *Phys. Rev. A* **3**, 1735 (1971).
- [3] M. Gross and S. Haroche, Superradiance: An essay on the theory of collective spontaneous emission, *Phys. Rep.* **93**, 301 (1982).
- [4] M. G. Benedict, A. M. Ermolaev, V. A. Malyshev, I. V. Sokolov, and E. D. Trifonov, *Super-radiance: Multiatomic Coherent Emission* (CRC Press, 1996).
- [5] N. Skribanowitz, I. P. Herman, J. C. MacGillivray, and M. S. Feld, Observation of Dicke superradiance in optically pumped HF gas, *Phys. Rev. Lett.* **30**, 309 (1973).
- [6] J. M. Raimond, P. Goy, M. Gross, C. Fabre, and S. Haroche, Collective absorption of blackbody radiation by Rydberg atoms in a cavity: An experiment on Bose statistics and Brownian motion, *Phys. Rev. Lett.* **49**, 117 (1982).
- [7] S. Inouye, A. P. Chikkatur, D. M. Stamper-Kurn, J. Stenger, D. E. Pritchard, and W. Ketterle, Superradiant Rayleigh scattering from a Bose-Einstein condensate, *Science* **285**, 571 (1999).
- [8] M. Scheibner, T. Schmidt, L. Worschech, A. Forchel, G. Bacher, T. Passow, and D. Hommel, Superradiance of quantum dots, *Nature Physics* **3**, 106 (2007).
- [9] S. Slama, S. Bux, G. Krenz, C. Zimmermann, and P. W. Courteille, Superradiant Rayleigh scattering and collective atomic recoil lasing in a ring cavity, *Phys. Rev. Lett.* **98**, 053603 (2007).
- [10] G. Rainò, M. A. Becker, M. I. Bodnarchuk, R. F. Mahrt, M. V. Kovalenko, and T. Stöferle, Superfluorescence from lead halide perovskite quantum dot superlattices, *Nature* **563**, 671 (2018).
- [11] G. Ferioli, A. Glicenstein, F. Robicheaux, R. T. Sutherland, A. Browaeys, and I. Ferrier-Barbut, Laser driven superradiant ensembles of two-level atoms near Dicke’s

- regime, arXiv:2107.13392 (2021).
- [12] C. J. Mewton and Z. Ficek, Radiative properties of a linear chain of coupled qubits, *J. Phys. B* **40** (2007).
- [13] H. Zoubi and H. Ritsch, Metastability and directional emission characteristics of excitons in 1D optical lattices, *Europhys. Lett.* **90**, 23001 (2010).
- [14] R. T. Sutherland and F. Robicheaux, Collective dipole-dipole interactions in an atomic array, *Phys. Rev. A* **94**, 013847 (2016).
- [15] S.-T. Chui, S. Du, and G.-B. Jo, Subwavelength transportation of light with atomic resonances, *Phys. Rev. A* **92**, 053826 (2015).
- [16] A. Asenjo-Garcia, M. Moreno-Cardoner, A. Albrecht, H. J. Kimble, and D. E. Chang, Exponential improvement in photon storage fidelities using subradiance and “selective radiance” in atomic arrays, *Phys. Rev. X* **7**, 031024 (2017).
- [17] J. A. Needham, I. Lesanovsky, and B. Olmos, Subradiance-protected excitation transport, *New J. Phys.* **21**, 073061 (2019).
- [18] S. J. Masson and A. Asenjo-Garcia, Atomic-waveguide quantum electrodynamics, *Phys. Rev. Research* **2**, 043213 (2020).
- [19] T. L. Patti, D. S. Wild, E. Shahmoon, M. D. Lukin, and S. F. Yelin, Controlling interactions between quantum emitters using atom arrays, *Phys. Rev. Lett.* **126**, 223602 (2021).
- [20] K. Brechtelsbauer and D. Malz, Quantum simulation with fully coherent dipole-dipole interactions mediated by three-dimensional subwavelength atomic arrays, *Phys. Rev. A* **104**, 013701 (2021).
- [21] D. Castells-Graells, D. Malz, C. C. Rusconi, and J. I. Cirac, Atomic waveguide QED with atomic dimers, arXiv:2107.10813 (2021).
- [22] G. Facchinetti, S. D. Jenkins, and J. Ruostekoski, Storing light with subradiant correlations in arrays of atoms, *Phys. Rev. Lett.* **117**, 243601 (2016).
- [23] M. T. Manzoni, M. Moreno-Cardoner, A. Asenjo-Garcia, J. V. Porto, A. V. Gorshkov, and D. E. Chang, Optimization of photon storage fidelity in ordered atomic arrays, *New J. Phys.* **20**, 083048 (2018).
- [24] S. Krämer, L. Ostermann, and H. Ritsch, Optimized geometries for future generation optical lattice clocks, *EPL (Europhysics Letters)* **114**, 14003 (2016).
- [25] L. Henriët, J. S. Douglas, D. E. Chang, and A. Albrecht, Critical open-system dynamics in a one-dimensional optical-lattice clock, *Phys. Rev. A* **99**, 023802 (2019).
- [26] W. S. Bakr, A. Peng, M. E. Tai, R. Ma, J. Simon, J. I. Gillen, S. Fölling, L. Pollet, and M. Greiner, Probing the superfluid-to-Mott insulator transition at the single-atom level, *Science* **329**, 547 (2010).
- [27] J. F. Sherson, C. Weitenberg, M. Endres, M. Cheneau, I. Bloch, and S. Kuhr, Single-atom-resolved fluorescence imaging of an atomic Mott insulator, *Nature* **467**, 68 (2010).
- [28] H. Kim, W. Lee, H.-G. Lee, H. Jo, Y. Song, and J. Ahn, In situ single-atom array synthesis using dynamic holographic optical tweezers, *Nat. Commun.* **7**, 13317 (2016).
- [29] M. Endres, H. Bernien, A. Keesling, H. Levine, E. R. Anschuetz, A. Krajenbrink, C. Senko, V. Vuletic, M. Greiner, and M. D. Lukin, Atom-by-atom assembly of defect-free one-dimensional cold atom arrays, *Science* **354**, 1024 (2016).
- [30] D. Barredo, S. de Léséleuc, V. Lienhard, T. Lahaye, and A. Browaeys, An atom-by-atom assembler of defect-free arbitrary two-dimensional atomic arrays, *Science* **354**, 1021 (2016).
- [31] A. Kumar, T.-Y. Wu, F. Giraldo, and D. S. Weiss, Sorting ultracold atoms in a three-dimensional optical lattice in a realization of Maxwell’s demon, *Nature* **561**, 83 (2018).
- [32] M. A. Norcia, A. W. Young, and A. M. Kaufman, Microscopic control and detection of ultracold strontium in optical-tweezer arrays, *Phys. Rev. X* **8**, 041054 (2018).
- [33] S. Saskin, J. T. Wilson, B. Grinkemeyer, and J. D. Thompson, Narrow-line cooling and imaging of ytterbium atoms in an optical tweezer array, *Phys. Rev. Lett.* **122**, 143002 (2019).
- [34] D. Ohl de Mello, D. Schäffner, J. Werkmann, T. Preuschoff, L. Kohfahl, M. Schlosser, and G. Birkel, Defect-free assembly of 2D clusters of more than 100 single-atom quantum systems, *Phys. Rev. Lett.* **122**, 203601 (2019).
- [35] R. J. Bettles, S. A. Gardiner, and C. S. Adams, Enhanced optical cross section via collective coupling of atomic dipoles in a 2D array, *Phys. Rev. Lett.* **116**, 103602 (2016).
- [36] E. Shahmoon, D. S. Wild, M. D. Lukin, and S. F. Yelin, Cooperative resonances in light scattering from two-dimensional atomic arrays, *Phys. Rev. Lett.* **118**, 113601 (2017).
- [37] J. Rui, D. Wei, A. Rubio-Abadal, S. Hollerith, J. Zeiher, D. M. Stamper-Kurn, C. Gross, and I. Bloch, A subradiant optical mirror formed by a single structured atomic layer, *Nature* **583**, 369 (2020).
- [38] A. Glicenstein, G. Ferioli, N. Šibalić, L. Brossard, I. Ferrier-Barbut, and A. Browaeys, Collective shift in resonant light scattering by a one-dimensional atomic chain, *Phys. Rev. Lett.* **124**, 253602 (2020).
- [39] R. Friedberg, S. R. Hartmann, and J. T. Manassah, Limited superradiant damping of small samples, *Phys. Lett. A* **40**, 365 (1972).
- [40] B. Coffey and R. Friedberg, Effect of short-range coulomb interaction on cooperative spontaneous emission, *Phys. Rev. A* **17**, 1033 (1978).
- [41] C. R. Stroud, J. H. Eberly, W. L. Lama, and L. Mandel, Superradiant effects in systems of two-level atoms, *Phys. Rev. A* **5**, 1094 (1972).
- [42] R. Friedberg and S. R. Hartmann, Superradiant stability in specially shaped small samples, *Opt. Commun.* **10**, 298 (1974).
- [43] G. Banfi and R. Bonifacio, Superfluorescence and cooperative frequency shift, *Phys. Rev. A* **12**, 2068 (1975).
- [44] S. J. Masson, I. Ferrier-Barbut, L. A. Orozco, A. Browaeys, and A. Asenjo-Garcia, Many-body signatures of collective decay in atomic chains, *Phys. Rev. Lett.* **125**, 263601 (2020).
- [45] S. J. Masson and A. Asenjo-Garcia, Universality of Dicke superradiance in arrays of quantum emitters, arXiv:2106.02042 (2021).
- [46] T. Gruner and D.-G. Welsch, Green-function approach to the radiation-field quantization for homogeneous and inhomogeneous Kramers-Kronig dielectrics, *Phys. Rev. A* **53**, 1818 (1996).
- [47] H. T. Dung, L. Knöll, and D.-G. Welsch, Resonant dipole-dipole interaction in the presence of dispersing and absorbing surroundings, *Phys. Rev. A* **66**, 063810 (2002).
- [48] H. J. Carmichael and K. Kim, A quantum trajectory un-

- raveling of the superradiance master equation, *Opt. Commun.* **179**, 417 (2000).
- [49] J. P. Clemens, L. Horvath, B. C. Sanders, and H. J. Carmichael, Collective spontaneous emission from a line of atoms, *Phys. Rev. A* **68**, 023809 (2003).
- [50] See Supplemental Material for further details on the algorithm used to calculate  $g^{(2)}(0)$  and derivations for  $N \rightarrow \infty$  in 1D and 2D, including Ref. [66].
- [51] G. Nienhuis and F. Schuller, Spontaneous emission and light scattering by atomic lattice models, *J. Phys. B* **20**, 23 (1987).
- [52] R. J. Bettles, S. A. Gardiner, and C. S. Adams, Cooperative eigenmodes and scattering in one-dimensional atomic arrays, *Phys. Rev. A* **94**, 043844 (2016).
- [53] F. Robicheaux and D. A. Suresh, Beyond lowest order mean-field theory for light interacting with atom arrays, *Phys. Rev. A* **104**, 023702 (2021).
- [54] O. Rubies-Bigorda and S. F. Yelin, Superradiance and subradiance in inverted atomic arrays, arXiv:2110.11288 (2021).
- [55] F. Robicheaux, Theoretical study of early time superradiance for atom clouds and arrays, arXiv:2110.00498 (2021).
- [56] C. Palacios-Berraquero, D. M. Kara, A. R. P. Montblanch, M. Barbone, P. Latawiec, D. Yoon, A. K. Ott, M. Loncar, A. C. Ferrari, and M. Atatüre, Large-scale quantum-emitter arrays in atomically thin semiconductors, *Nat. Commun.* **8**, 15093 (2017).
- [57] N. V. Proscia, Z. Shotan, H. Jayakumar, P. Reddy, C. Cohen, M. Dollar, A. Alkauskas, M. Doherty, C. A. Meriles, and V. M. Menon, Near-deterministic activation of room-temperature quantum emitters in hexagonal boron nitride, *Optica* **5**, 1128 (2018).
- [58] C. Li, N. Mendelson, R. Ritika, Y. Chen, Z.-Q. Xu, M. Toth, and I. Aharonovich, Scalable and deterministic fabrication of quantum emitter arrays from hexagonal boron nitride, *Nano Lett.* **21**, 3626 (2021).
- [59] T. Kornher, K. Xia, R. Kolesov, N. Kukharchyk, R. Reuter, P. Siyushev, R. Stöhr, M. Schreck, H.-W. Becker, B. Villa, A. D. Wieck, and J. Wrachtrup, Production yield of rare-earth ions implanted into an optical crystal, *Appl. Phys. Lett.* **108**, 053108 (2016).
- [60] A. Sipahigil, R. E. Evans, D. D. Sukachev, M. J. Burek, J. Borregaard, M. K. Bhaskar, C. T. Nguyen, J. L. Pacheco, H. A. Atikian, C. Meuwly, R. M. Camacho, F. Jelezko, E. Bielejec, H. Park, M. Lončar, and M. D. Lukin, An integrated diamond nanophotonics platform for quantum-optical networks, *Science* **354**, 847 (2016).
- [61] G.-D. Lin and S. F. Yelin, Superradiance in spin- $j$  particles: Effects of multiple levels, *Phys. Rev. A* **85**, 033831 (2012).
- [62] R. T. Sutherland and F. Robicheaux, Superradiance in inverted multilevel atomic clouds, *Phys. Rev. A* **95**, 033839 (2017).
- [63] A. Piñeiro Orioli, J. K. Thompson, and A. M. Rey, Emergent dark states from superradiant dynamics in multi-level atoms in a cavity, arXiv:2106.00019 (2021).
- [64] A. Goban, C.-L. Hung, J. D. Hood, S.-P. Yu, J. A. Muniz, O. Painter, and H. J. Kimble, Superradiance for atoms trapped along a photonic crystal waveguide, *Phys. Rev. Lett.* **115**, 063601 (2015).
- [65] P. Solano, P. Barberis-Blostein, F. K. Fatemi, L. A. Orozco, and S. L. Rolston, Super-radiance reveals infinite-range dipole interactions through a nanofiber, *Nat. Commun.* **8**, 1857 (2017).
- [66] J. Wilkinson, *The Algebraic Eigenvalue Problem* (Clarendon Press, Oxford, 1965).

**SUPPLEMENTAL MATERIAL: DICKE SUPERRADIANCE IN ORDERED LATTICES: ROLE OF GEOMETRY AND DIMENSIONALITY**

**1. Revivals in  $g^{(2)}(0)$**

As discussed in the main text, while the variance generally decreases with interatomic distance  $d$ , there are “revivals” at particular distances. In 1D, these occur at  $d = n\lambda_0/2$ , where  $n \in \mathbb{N}$  and  $\lambda_0$  is the wavelength of the atomic transition. In 2D and 3D, there are also geometric resonances associated with displacements non-orthogonal to the lattice, and revivals occur more frequently with increasing  $d$ . These can be seen in Fig 5, where  $g^{(2)}(0)$  starts to rise with increasing  $d$  at these resonances.

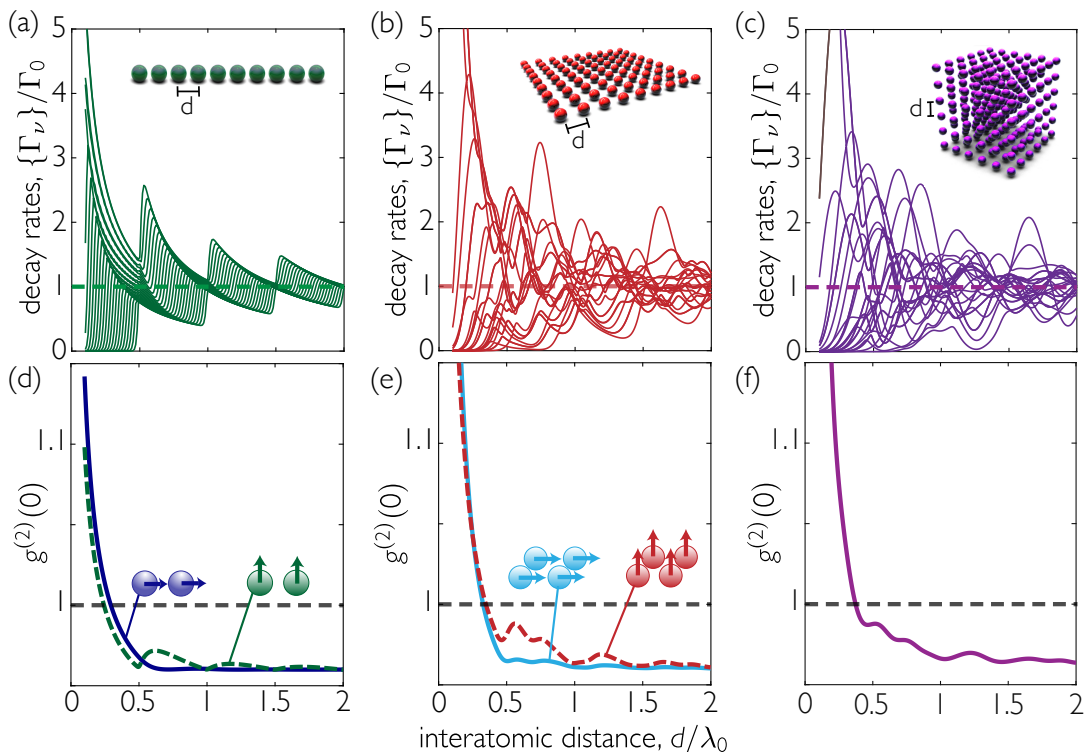


FIG. 5. Collective decay rates (a-c) and second order correlation function  $g^{(2)}(0)$  (d-f) as a function of interatomic distance  $d$  for atomic arrays of different dimensions. In (a,d),  $N = 25$  atoms form a 1D array, and the transition polarization is either perpendicular (green) or parallel (blue) to the chain. In (b,e),  $N = 5^2 = 25$  atoms form a 2D lattice with polarization axis in-plane (red) and out-of-plane (light blue). In (c,f),  $N = 3^3 = 27$  atoms are arranged in a 3D lattice, with polarization axis aligned with one of the main axes of the array. In all plots, horizontal lines are guides to the eye.

**2. Calculating the variance of the decay rates in  $O(N)$  steps**

Here we present the algorithm that allows us to find the variance of the decay rates in  $O(N)$  steps, instead of the  $O(N^3)$  scaling that would result from employing common algorithms to find the eigenvalues of an  $N \times N$  matrix [66]. Let  $\mathbf{A}$  be the normalized matrix  $\mathbf{\Gamma}/\Gamma_0$  with components  $A_{ij}$  and eigenvalues  $\{\lambda_i\}$ . The matrix  $\mathbf{A}$  inherits symmetry properties from the Green’s tensor. Due to reciprocity,  $G_{\alpha\beta}(\mathbf{r}_i, \mathbf{r}_j, \omega_0) = G_{\beta\alpha}(\mathbf{r}_j, \mathbf{r}_i, \omega_0)$  and since all atoms share a common quantization axis,  $\alpha = \beta$  for all  $i, j$ . Therefore,  $\mathbf{A}$  is real and symmetric. The diagonal elements of  $\mathbf{\Gamma}$  correspond to the single atom decay rate ( $\Gamma^{ii} = \Gamma_0$ ) such that

$$\text{Tr } \mathbf{A} = \sum_{i=1}^N \lambda_i = N. \quad (11)$$

Let  $\mathbf{D}$  be the diagonalization of  $\mathbf{A}$  such that  $\mathbf{A} = \mathbf{PDP}^{-1}$  (the spectral theorem ensures  $\mathbf{A}$  can be diagonalized as it is real and symmetric), with  $\mathbf{D}$  being a diagonal matrix with diagonal elements  $\lambda_1, \dots, \lambda_N$ . Therefore,

$$\mathbf{D}^2 = \begin{pmatrix} \lambda_1^2 & & \\ & \ddots & \\ & & \lambda_N^2 \end{pmatrix}, \quad (12)$$

with the trace of  $\mathbf{D}^2$  being all we need to obtain  $g^{(2)}(0)$ . Since

$$\mathbf{A}^2 = \mathbf{PDP}^{-1}\mathbf{PDP}^{-1} = \mathbf{PD}^2\mathbf{P}^{-1}, \quad (13)$$

we only need to calculate the trace of  $\mathbf{A}^2$ , since  $\text{Tr } \mathbf{A}^2 = \text{Tr } \mathbf{D}^2$ . Multiplying matrices is computationally costly, but we can avoid that operation by realizing that

$$\text{Tr } \mathbf{A}^2 = \sum_{i=1}^N \left( \sum_{j=1}^N A_{ij} A_{ji} \right) = \sum_{i,j=1}^N A_{ij}^2, \quad (14)$$

as  $\mathbf{A}$  is real and symmetric. The sum of squared decay rates is then

$$\sum_{\nu=1}^N \left( \frac{\Gamma_{\nu}}{\Gamma_0} \right)^2 = \sum_{i,j=1}^N \left( \frac{\Gamma^{ij}}{\Gamma_0} \right)^2 = N + 2 \sum_{i=1, j>i}^N \left( \frac{\Gamma^{ij}}{\Gamma_0} \right)^2 = N + 2 \sum_{\beta} n_{\beta} \left( \frac{\Gamma_{\beta}}{\Gamma_0} \right)^2, \quad (15)$$

where we sum over all different displacement vectors  $\{\mathbf{s}_{\beta}\}$ ,  $\Gamma_{\beta}$  is the dissipative interaction rate between atoms separated by displacement vector  $\mathbf{s}_{\beta}$ , and  $n_{\beta}$  is the number of repetitions of  $\mathbf{s}_{\beta}$  in the array. For arbitrary geometries (where all vectors are unique), this scales as  $O(N^2)$ . However, in ordered arrays, the multiplicity of most displacement vectors is larger than one (for example, in a 1D array,  $\mathbf{s}_2 \equiv \mathbf{r}_{1,3} = \mathbf{r}_{2,4} = -\mathbf{r}_{5,3} = \dots$ ). This reduces the complexity of calculating the sum of squared decay rates to the number of different displacement vectors.

In ordered arrays, the sum in  $\beta$  has  $O(N)$  terms and  $g^{(2)}(0)$  is calculated in  $O(N)$  steps. The atoms occupy a grid such that all displacement vectors can be expressed as integer numbers of discrete steps in each dimension. To this end, we define a dimensionless vector  $\mathbf{d}_{\beta} = \{a_{\beta}, b_{\beta}, c_{\beta}\}$  with  $a_{\beta}, b_{\beta}, c_{\beta}$  such that  $\mathbf{s}_{\beta} = a_{\beta}\hat{\mathbf{s}}_1 + b_{\beta}\hat{\mathbf{s}}_2 + c_{\beta}\hat{\mathbf{s}}_3$  with  $\hat{\mathbf{s}}_{1,2,3}$  the three vectors that describe the unit cell. We define  $N_{1D}$  as the number of atoms along a one-dimensional slice in the array: in 1D  $N_{1D} = N$  and  $b_{\beta} = c_{\beta} = 0$ , in 2D  $N_{1D} = \sqrt{N}$  and  $c_{\beta} = 0$ , and in 3D  $N_{1D} = \sqrt[3]{N}$ .

*Counting in 1D*– All displacement vectors can be identified by considering one end atom. The shortest displacement vector is that of nearest neighbors:  $|\mathbf{d}_{\beta}| = 1$ . This appears  $N - 1$  times, as  $\mathbf{r}_{1,2} = \mathbf{r}_{2,3} = \dots = \mathbf{r}_{N-1,N}$ . The largest displacement vector is that between the two end atoms,  $|\mathbf{d}_{\beta}| = N - 1$ , which appears only once. More generally, a displacement vector of  $a_{\beta}$  is repeated  $n_{\beta} = N_{1D} - a_{\beta}$  times.

*Counting in 2D*– All displacement vectors can be identified by considering two adjacent corners. The displacement vectors between the first corner and all other atoms provides all displacement vectors of the form  $\mathbf{d}_{\beta} = \{a_{\beta}, b_{\beta}\}$  with  $0 \leq a_{\beta}, b_{\beta} \leq N_{1D} - 1$  (excluding  $\{0, 0\}$ , which are counted in the factor of  $N$  in Eq. (15)). However, this does not include vectors where  $a_{\beta}$  (or equivalently  $b_{\beta}$ ) are negative. For example, in Fig. 6, displacements from the bottom left corner yield  $\mathbf{d}_{\alpha}$  and  $\mathbf{d}_{\gamma}$ , but they do not include  $\mathbf{d}_{\xi}$ . To complete the set of possible displacement vectors we require those given by a second-corner:  $\mathbf{d}_{\beta} = \{a_{\beta}, -b_{\beta}\}$  (or equivalently  $\mathbf{d}_{\beta} = \{-a_{\beta}, b_{\beta}\}$ , depending on the choice of corner) with  $1 \leq a_{\beta}, b_{\beta} \leq N_{1D} - 1$ . Note that here  $a_{\beta}, b_{\beta} \neq 0$ , since those vectors are already included in those defined by the first corner. To count repetitions, we note that, as in 1D, a vector which covers  $a_{\beta}$  sites in the first dimension fits  $N_{1D} - a_{\beta}$  times. The same holds for the second dimension so the total repetitions is

$$n_{\beta} = (N_{1D} - a_{\beta})(N_{1D} - b_{\beta}). \quad (16)$$

*Counting in 3D*– All displacement vectors can be identified by considering the four corners of one face. As in 2D, the first corner provides all displacement vectors of the form  $\mathbf{d}_{\beta} = \{a_{\beta}, b_{\beta}, c_{\beta}\}$  with  $0 \leq a_{\beta}, b_{\beta}, c_{\beta} \leq N_{1D} - 1$  (again excluding  $\{0, 0, 0\}$ ). The other three corners provide the rest of the set, with care being taken to not repeat vectors. The number of repetitions is then

$$n_{\beta} = (N_{1D} - a_{\beta})(N_{1D} - b_{\beta})(N_{1D} - c_{\beta}). \quad (17)$$

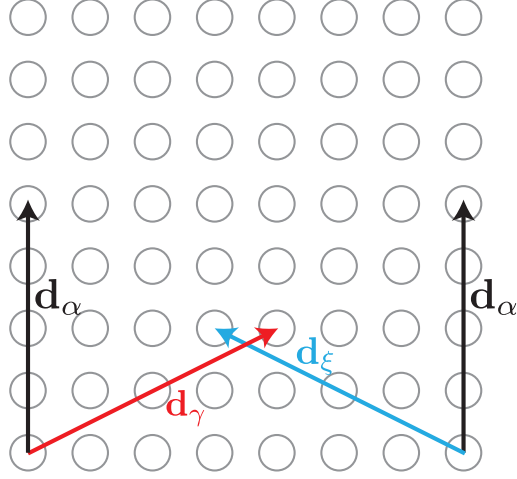


FIG. 6. Schematic of different displacement vectors in a square lattice.

### 3. Calculations for infinite arrays

Building on the expression for the second order correlation function of a finite array,

$$g^{(2)}(0) = 1 - \frac{2}{N} + \frac{1}{N^2} \sum_{\nu=1}^N \left( \frac{\Gamma_{\nu}}{\Gamma_0} \right)^2, \quad (18)$$

and making the prescription

$$\sum_{\nu=1}^N \rightarrow N \left( \frac{d}{2\pi} \right)^n \int d\mathbf{k}, \quad (19)$$

where  $n$  is the number of dimensions of the array and the vector  $\mathbf{k}$  has  $n$  components, we find the expression for  $g^{(2)}(0)$  of an infinite array (in the limit  $N \rightarrow \infty$ ):

$$g^{(2)}(0) = 1 + \frac{1}{N} \left[ -2 + \left( \frac{d}{2\pi} \right)^n \int d\mathbf{k} \frac{\Gamma(\mathbf{k})^2}{\Gamma_0^2} \right]. \quad (20)$$

The condition for a superradiant burst is therefore

$$\frac{1}{2} \left( \frac{d}{2\pi} \right)^n \int d\mathbf{k} \left( \frac{\Gamma(\mathbf{k})}{\Gamma_0} \right)^2 > 1. \quad (21)$$

#### 3.1 1D arrays with $d < 0.5\lambda_0$

As written in the main text, the decay rates for an infinite array read

$$\frac{\Gamma_{1D,\perp}(k_z)}{\Gamma_0} = \frac{3\pi}{4k_0d} \sum_{g_z} \left( 1 + \frac{(k_z + g_z)^2}{k_0^2} \right), \quad (22a)$$

$$\frac{\Gamma_{1D,\parallel}(k_z)}{\Gamma_0} = \frac{3\pi}{2k_0d} \sum_{g_z} \left( 1 - \frac{(k_z + g_z)^2}{k_0^2} \right), \quad (22b)$$

where the summations run over reciprocal lattice vectors  $g_z = n2\pi/d \forall n \in \mathbb{Z}$  that satisfy the condition  $|g_z + k_z| \leq k_0$ . Here, we consider  $d/\lambda_0 < 0.5$ , where all non-zero decay rates are contained within the first Brillouin zone and the only non-zero term in the sum is  $g_z = 0$ .

Performing the integrals in  $k$ -space for both polarizations, we find

$$\int_{BZ1} dk_z \left( \frac{\Gamma_{1D,\perp}(k_z)}{\Gamma_0} \right)^2 = \frac{21}{40k_0} \left( \frac{2\pi}{d} \right)^2, \quad (23a)$$

$$\int_{BZ1} dk_z \left( \frac{\Gamma_{1D,\parallel}(k_z)}{\Gamma_0} \right)^2 = \frac{3}{5k_0} \left( \frac{2\pi}{d} \right)^2. \quad (23b)$$

The second order correlation function is then

$$g_{1D,\perp}^{(2)}(0) = 1 + \frac{1}{N} \left( \frac{21\lambda_0}{40d} - 2 \right), \quad (24a)$$

$$g_{1D,\parallel}^{(2)}(0) = 1 + \frac{1}{N} \left( \frac{3\lambda_0}{5d} - 2 \right). \quad (24b)$$

Imposing the condition  $g^{(2)}(0) = 1$  yields the critical distances of Eq. (7) in the main text.

### 3.2 1D arrays with $d > 0.5\lambda_0$

Here we demonstrate that the critical distances that we have found in the previous section are the only possible ones. For  $0.5 < d/\lambda_0 < 1$ , there are three possible values of  $g_z = \{-2\pi/d, 0, 2\pi/d\}$  that contribute to the decay rates. The integrals of the square of the decay rates for both polarizations yield

$$\begin{aligned} \int_{BZ1} \left( \frac{\Gamma_{1D,\perp}(k_z)}{\Gamma_0} \right)^2 dk_z &= \frac{9\pi^2}{16k_0^2 d^2} \int_{-\pi/d}^{\pi/d} \sum_{g_z} \left( 1 + \frac{(k_z + g_z)^2}{k_0^2} \right)^2 + \sum_{g_z \neq g'_z} \left( 1 + \frac{(k_z + g_z)^2}{k_0^2} \right) \left( 1 + \frac{(k_z + g'_z)^2}{k_0^2} \right) dk_z \\ &= \frac{2\pi^2}{k_0 d^2} \left( -\frac{3\lambda_0^5}{5d^5} - \frac{3\lambda_0^3}{d^3} + \frac{6\lambda_0^2}{d^2} - \frac{9\lambda_0}{2d} + \frac{63}{20} \right), \end{aligned} \quad (25a)$$

$$\int_{BZ1} \left( \frac{\Gamma_{1D,\parallel}(k_z)}{\Gamma_0} \right)^2 dk_z = \frac{2\pi^2}{k_0 d^2} \left( -\frac{12\lambda_0^5}{5d^5} + \frac{12\lambda_0^3}{d^3} - \frac{12\lambda_0^2}{d^2} - \frac{18}{5} \right). \quad (25b)$$

These expressions do not satisfy the minimal condition for a superradiant burst [i.e., Eq. (21)] anywhere in the region  $0.5 < d/\lambda_0 < 1$ .

For larger interatomic separations, we can upper bound the integral to prove that  $g^{(2)}(0) < 1$  always. For perpendicular polarization we bound the double sum by

$$\sum_{g_z, g'_z} \left( 1 + \frac{(k_z + g_z)^2}{k_0^2} \right) \left( 1 + \frac{(k_z + g'_z)^2}{k_0^2} \right) < \sum_{g_z} \left( 1 + \frac{(k_z + g_z)^2}{k_0^2} \right)^2 + 2N_g \left( 1 + \frac{(k_z + g_z)^2}{k_0^2} \right)^2, \quad (26)$$

where  $N_{g_z}$  is a natural number such that  $g_z = \pm N_g 2\pi/d$ . The inequality is produced by upper bounding each of the products in the sum as the square of whichever term is larger. This allows us to bound the integral as

$$\int_{BZ1} \left( \frac{\Gamma_{1D,\perp}(k_z)}{\Gamma_0} \right)^2 dk_z < \frac{21\pi^2}{5k_0 d^2} + \frac{63\pi}{48d}, \quad (27)$$

which satisfies the condition for a superradiant burst for  $d/\lambda_0 < 0.7814$ . Since we have already shown that the superradiant burst cannot be exhibited for 1D arrays with  $0.2625 < d/\lambda_0 < 1$ , this means that  $d < 0.2625\lambda_0$  is the only region a superradiant burst can be produced.

Similarly, for parallel polarization we bound the integral by

$$\int_{BZ1} \left( \frac{\Gamma_{1D,\parallel}(k_z)}{\Gamma_0} \right)^2 dk_z < \frac{24\pi^2}{5k_0 d^2} + \frac{3\pi}{4d}, \quad (28)$$

which satisfies the condition for a superradiant burst if  $d/\lambda_0 < 0.8571$ . Again, we have shown previously that a superradiant burst cannot be produced for  $0.3 < d/\lambda_0 < 1$  such that  $d < 0.3\lambda_0$  is the only region a superradiant burst can be produced.

## 3.3 2D arrays

Recalling from the main text, the decay rates in 2D are given by

$$\frac{\Gamma_{2D,\perp}(\mathbf{k})}{\Gamma_0} = \frac{3\pi}{k_0^3 d^2} \sum_{\mathbf{g}} \frac{|\mathbf{k} + \mathbf{g}|^2}{\sqrt{k_0^2 - |\mathbf{k} + \mathbf{g}|^2}}, \quad (29a)$$

$$\frac{\Gamma_{2D,\parallel}(\mathbf{k})}{\Gamma_0} = \frac{3\pi}{k_0^3 d^2} \sum_{\mathbf{g}} \frac{k_0^2 - |(\mathbf{k} + \mathbf{g}) \cdot \boldsymbol{\rho}|^2}{\sqrt{k_0^2 - |\mathbf{k} + \mathbf{g}|^2}}, \quad (29b)$$

where the summations run over all reciprocal lattice vectors  $\mathbf{g} = \{n2\pi/d, m2\pi/d\} \forall n, m \in \mathbb{Z}$  that satisfy  $|\mathbf{k} + \mathbf{g}| \leq k_0$ . The integral is performed over all non-zero decay rates, which form a disc,  $D_{k_0}$ , centred on zero with radius  $k_0$ .

We first analyze the situation for  $d < 0.5\lambda_0$ . In this case, these rates entirely lie within the first Brillouin zone and the only possible terms are  $\mathbf{g} = \{0, 0\}$ . Integrating over the square of the decay rates yields

$$\int_{BZ1} \left( \frac{\Gamma_{2D,\perp}(\mathbf{k})}{\Gamma_0} \right)^2 d\mathbf{k} = \frac{9\pi\lambda_0^2}{2\pi d^4} \int_0^{k_0} \frac{k^5}{k_0^2 - k^2} dk, \quad (30a)$$

$$\int_{BZ1} \left( \frac{\Gamma_{2D,\parallel}(\mathbf{k})}{\Gamma_0} \right)^2 d\mathbf{k} = \frac{9\pi\lambda_0^2}{4d^4} \left( 1 + \frac{3}{4} \int_0^{k_0} \frac{k^5}{k_0^2 - k^2} dk \right). \quad (30b)$$

In both cases the integral diverges as  $|\mathbf{k}| \rightarrow k_0$ , breaking the analytical character of the approach. Nevertheless, we can characterize the scaling of the divergence with atom number. The integral scales as

$$\int_0^{k_0(1-\varepsilon)} \frac{k^5}{k_0^2 - k^2} \approx \alpha k_0^4 \log \frac{1}{\varepsilon}, \quad (31)$$

where  $\varepsilon$  introduces a small deviation from  $|\mathbf{k}| = k_0$ . A finite array will sample the first Brillouin zone at a rate given by  $1/\sqrt{N}$  so we take  $\varepsilon = 1/\sqrt{N}$ .

As we approach the infinite limit, the second order correlation function scales with atom number as:

$$g_{2D,\perp}^{(2)}(0) \approx 1 + \frac{1}{N} \left( \frac{9\lambda_0^2}{8\pi d^2} \alpha \log \sqrt{N} - 2 \right), \quad (32a)$$

$$g_{2D,\parallel}^{(2)}(0) \approx 1 + \frac{1}{N} \left( \frac{9\lambda_0^2}{16\pi d^2} + \frac{27\lambda_0^2}{64\pi d^2} \alpha \log \sqrt{N} - 2 \right). \quad (32b)$$

Setting  $g^{(2)}(0) = 1$  yields the critical distance for each polarization (written in the main text).

While our analysis focuses on  $d < 0.5\lambda_0$ , the same type divergence occurs whenever  $|\mathbf{k} + \mathbf{g}| \rightarrow k_0$ . Therefore, we expect the scaling of the critical distance with atom number to be sub-logarithmic as well in those cases.